Advanced Engineering Informatics 29 (2015) 459–471

Contents lists available at ScienceDirect

Advanced Engineering Informatics

journal homepage: www.elsevier.com/locate/aei

Dynamic equipment workspace generation for improving earthwork safety using real-time location system

Faridaddin Vahdatikhaki [a,1], Amin Hammad [b,*]

[a] Building, Civil and Environmental Engineering Department, Concordia University, 1455 De Maisonneuve Blvd. West, Montreal, Quebec H3G 1M8, Canada
[b] Concordia Institute for Information Systems Engineering, 1455 De Maisonneuve Blvd. West, Montreal, Quebec H3G 1M8, Canada

ARTICLE INFO

Article history:
Received 22 September 2014
Received in revised form 24 February 2015
Accepted 10 March 2015
Available online 7 April 2015

Keywords:
Dynamic equipment workspace
Earthwork equipment
Real-time location systems

ABSTRACT

Earthwork equipment accounts for a large proportion of the fatalities on construction sites. According to the U.S. Bureau of Labor Statistics, in the period between 1992 and 2002, struck by vehicles and struck by objects (e.g., vehicle parts, vehicle loads, or falling vehicles) were identified as the causes of 30% and 24% of fatal equipment-related accidents on excavations sites, respectively. It is therefore of a paramount importance to improve the safety of construction sites by increasing the peripheral awareness of the operators of earthwork equipment. Several research works have investigated numerous collision avoidance systems that exploit real-time location systems and proximity measurements to mitigate the risk of accidents on excavation sites. However, these systems often detect collisions based on using the workspaces that only account for the geometry and the degrees of freedom of the equipment, and thus disregard the state-dependent characteristics of equipment. This results in reserving a large space for every piece of equipment, which reduces the applicability of these systems in congested sites. Therefore, this paper proposes a novel method for generating dynamic equipment workspaces based on the continuous monitoring of a spectrum of equipment-related information, i.e., the current pose/state of the equipment, and the speed characteristics of each movement. This method uses the required operation stoppage time to determine how much space needs to be reserved for each piece of equipment. A case study is conducted to validate the proposed method. It is shown that the proposed method has a strong potential in capturing the hazardous areas around the equipment and triggering warnings in view of the impending movements of various pieces of equipment. Also, the proposed method proved to have potential applications in actual projects in congested sites where space is limited.

1. Introduction

With only less than 5% of the U.S. work force, the construction industry claims around 20% of fatalities and injuries in workplaces [30]. In the U.K., in addition to 25,000–30,000 injured, approximately 1500 people are losing their lives on construction sites in a typical decade [15]. Earthwork equipment accounts for a large share of injuries on construction sites. According to Hinze and Teizer [25], one-fourth of construction fatalities are due to equipment-related incidents. 52.6% of reported deaths in the excavation work between 1992 and 2002 involved vehicles [34]. Equipment-related incidents are usually categorized into struck-by and caught-in/between accidents [24]. In the U.S., 428 equipment-related struck-by and caught-in/between accidents were reported between 1995 and 2008 [53]. In the U.K., of the total number of fatalities in a period of 7 years (1996–2003), 14% were identified to have been caused by being struck by a moving vehicle [26]. According to McCann [34], the reports from Bureau of Labor Statistics indicate that in the period between 1992 and 2002, the causes of 30%, 24% and 12% of fatal equipment-related accidents on excavations sites were identified to be struck by vehicles, struck by objects (e.g., vehicle parts, vehicle loads, or falling vehicles), and caught in/between, respectively. Among various types of equipment involved in struck-by accidents, truck and excavators are the most prevalent, together accounting for more than 50% of reported struck-by accidents between 1997 and 2000 [24]. Among those who fell victim to equipment-related fatal accidents in excavation work, 52% and 34% were the operators and workers on foot, respectively [34].

These statistics suggest that earthwork operations are in need of enhanced safety to avoid damages, injuries and fatalities. With this need in mind, many researchers have explored a wide range of solutions to mitigate the risk of accidents on excavation sites

* Corresponding author. Tel.: +1 (514) 848 2424x5800; fax: +1 (514) 848 3171.
E-mail addresses: f_vahdat@encs.concordia.ca (F. Vahdatikhaki), hammad@ciise.concordia.ca (A. Hammad).
[1] Tel.: +1 (514) 848 2424x7074; fax: +1 (514) 848 3171.

http://dx.doi.org/10.1016/j.aei.2015.03.002
1474-0346/

through reducing the possibility of collisions between equipment through a proper planning method [9,33,43,23,35]. These methods identify the spaces required for the safe completion of different activities, i.e., activity workspaces, and try to reduce the overlap between them.

Despite the effectiveness of these methods in reducing the possibility of collisions between different teams of equipment at a macro level, they are not fully capable of averting safety risks emanating from human errors and unforeseen circumstances. Additionally, space is a limited resource that many of earthwork projects do not have. These methods are not able to effectively improve the safety in congested sites, given that activity workspaces may overlap in many instances.

While there could be various different root causes behind the equipment-related fatalities, e.g., loss of attention, unsafe driving habits, distractions, visibility and blind spots, etc. [25], the majority of equipment-related accidents can be avoided if the dangerous areas around the equipment are monitored in real time and the operators are warned against any intrusions into these areas. As a result, it is of a paramount importance to devise a complementary real-time mechanism to reduce safety risks based on the current pose and state of the equipment. To this end, researchers considered systems that generate warning against dangerous proximities using radar-based proximity sensors [39,13], vision-based tracking [12], and Real-time Location Systems (RTLSs) such as the Global Positioning System (GPS), Radio Frequency Identification (RFID), and Ultra Wideband (UWB) [5,8,45,6,54,22,52,55]. These methods are applied at the monitoring phase with the intention to ensure that different pieces of equipment do not collide with one another. Similar to the methods used at the planning phase, these methods consider the space around the equipment that should not be trespassed by other equipment to avoid potential collision in the immediate future. Because these spaces are applied to equipment, as opposed to the activities, and their shapes are dynamically changing based on the current pose of the equipment, they are referred to as Dynamic Equipment Workspaces (DEWs) in this paper. The correlation between the two types of workspace is that an activity workspace must be the envelope that contains all the *DEWs* generated by the fleet assigned to that activity over the scheduled period. Although *DEWs* are alternatively termed in the literature as "safety envelopes" [5,55] or "safety zones" [40], the authors believe that, given the above correlation, it is preferable to use the unified term "workspaces" for both activity and equipment.

Nevertheless, to the best of the authors' knowledge, the existing methods for generating *DEW*s do not take full advantage of the combination of valuable pose, state, geometry, and speed characteristics of the equipment to accurately estimate the shape of *DEW*s. Consequently, the present research aims to leverage a set of information regarding the geometry, pose, state, and speed characteristics of the equipment to determine the shape and size of the workspace based on the required stoppage time of the equipment so as to secure the early identification of potential collisions while making a more economic use of space.

The structure of the paper is as follows. First, the previous relevant studies are presented. Then, the *DEW* generation method is elaborated. Next, a case study is elucidated as a means to validate the proposed method. Finally, the conclusions and future work are presented.

2. Literature review

2.1. DEWs related research

Two approaches can be found in the research addressing the generation of DEWs. While some researchers use only the equipment geometry and pose for the generation of DEWs, others also consider the speed characteristics of the equipment.

2.1.1. DEWs based on the equipment geometry and pose

Several methods have been developed to generate *DEWs* based on the application of different types of RTLSs. Generally, the methods of generating *DEWs* based on the proximity measurements can be categorized into two groups. Some methods are totally independent of the pose, state and speed data; and therefore they over-conservatively reserve the space within a radius (r) of the equipment (called here cylindrical workspace, Fig. 1(a)). For instance, CRC Mining [14] developed the Shovel Load Assist System that uses the combined data from a laser scanner, GPS and pulse radio to locate the trucks and dozers in the vicinity of the shovel to avoid the potential collision with them. There are many examples of cylindrical workspaces in previously proposed systems for collision avoidance on construction sites [7,45,11,32,31,37,29]. Other methods detect the shortest distance between the two pieces of equipment and use a minimum acceptable threshold for generating the warnings, which is equivalent to considering only the pose of the equipment and creating a buffer of width (b) around the equipment (called here buffer workspace, Fig. 1(b)). For instance, Kim et al. [28] proposed a method for real-time collision avoidance systems that uses laser range finders to model the obstacles on the site and then calculates the shortest distance of the equipment to various surrounding obstacles. If a threshold distance is violated, the warning is generated. A GPS-based collision avoidance system was developed by Wu et al. [52], with the central objective to assist crane operators with handling concrete buckets in a dam construction project. Talmaki and Kamat [42] proposed the application of hybrid virtuality for the simulation of the actual jobsite and detecting hazardous proximities between various objects using a combination of 3D CAD models, terrain models, GPS and sensory data, and input from a Geographic Information System (GIS). This method uses proximity measurements as the basis for the collision detection. Zolynski et al. [55] developed a two-layer safety mechanism for autonomous excavators that generates a safety buffer around the equipment based on the present pose of the equipment and avoids collisions with the surrounding objects using a laser scanner. Another instance of the methods that use buffer workspace is developed by Guenther and Salow [22].

However, as stated in Section 1, the cylindrical workspace reserves a large space for the safe performance of the equipment, considerably diminishing its effectiveness for the application in a

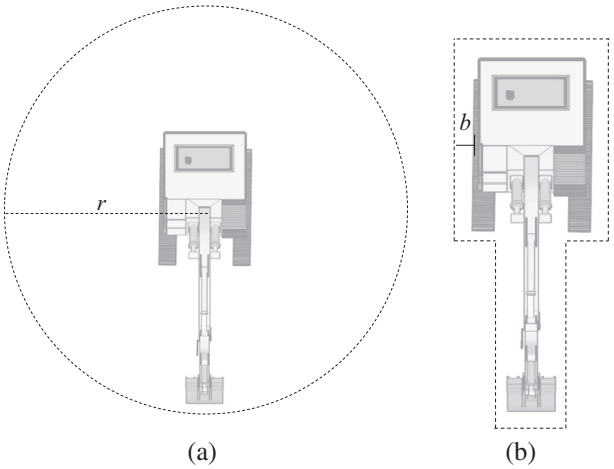

Fig. 1. (a) Cylindrical workspace, and (b) buffer workspace (the model of excavator is obtained from Google 3D Warehouse [21]).

congested site. On the other hand, while performing better in terms of economic use of space, the buffer workspace takes more time to detect potential collisions compared to the cylindrical workspace. In both cases, the shape of *DEW*s generated through these methods is determined by the Degrees of Freedom (DOFs) and the geometry of the equipment. Ignoring the movement characteristics of the equipment, i.e., the magnitude and direction of the instantaneous speed, results in reserving a large space around the equipment. However, a portion of this space can be safely used by other equipment if the workspace is defined more efficiently through considering the movement characteristics of the equipment.

2.1.2. DEWs based on the equipment geometry, pose, and speed characteristics

Other researchers have deployed the information pertinent to the equipment movement characteristics to enhance the proximity measurement with a degree of prediction about the possible states of the equipment in the near future. These methods do not only rely on the proximity between various equipment and objects as the indication of imminent hazards, but also use the movement characteristics of the equipment to foresee if the equipment is likely to engage in potentially risky situations if it follows its current trajectory. For instance, Burns [5] proposed a method for the generation of workspaces around autonomous equipment based on a set of characteristics such as the current position, trajectory vector, speed, and system tolerances.

Oloufa et al. [36] proposed a GPS-based collision avoidance system which is based on the simulation of potential collision through the analysis of equipment's motion vectors. A probabilistic approach was proposed by Worrall and Nebot [50] that uses the speed profiles of the equipment to account for the properties of the road network when detecting the impending vehicle intersection. Hukkeri [27] proposed a safety mechanism using intention mapping techniques in which every piece of equipment speculates the potential path of other mobile objects on the site and tries to avoid collisions. Zhang and Hammad [54] used UWB to track the movement of equipment, and further used the location data to create a buffer around the equipment based on its speed, which is in turn used to identify the potential collision between different pieces of equipment. Cheng [10] proposed to use the pose and speed data for the generation of the *DEW*. However, the proposed method does not consider the equipment state as a means to economize the use of space around the equipment and does not cover the equipment with rotary movements, e.g., excavators. In another instance, a GPS and Radio Frequency (RF) based collision avoidance system was developed by SAFEmine [40], where the speed characteristics and the pose of the equipment are used to generate the dynamic workspace of the equipment and generate warnings when workspaces of different pieces of equipment collide with one another. In a more recent work, Wang and Razavi [49] suggested considering the breaking distance, the reaction time, the equipment heading, and speed to create a workspace with a lower false alarm rate. Despite making a distinction between moving and static equipment, the method does not fully exploit the equipment state information (e.g., the mobile excavator can be in swinging or traversal states). Additionally, the adapted approach in this research treats equipment as a single point and disregards the geometry of the equipment.

In general, the existing methods do not distinguish between different states of the equipment when generating the workspaces. The valuable information about the state of the equipment can help better determine the size of the *DEW* in view of the potential dangers that may emanate not solely from the speed characteristics of the equipment but also from the nature of the equipment's current state. Therefore, it could be argued that if the combination of equipment geometry, current pose, state, and speed characteristics are properly leveraged, it is possible to economize the space usage without sacrificing the effectiveness of the collision detection.

2.2. Operation stoppage time

In order to determine the shape of *DEW*s based on the current pose, state and speed characteristics, the required stoppage time (t_s) of the operation is of a significant value. t_s can be used to determine how much of the space in the moving direction of the equipment is unsafe after the operator becomes aware of a potential collision. According to the definition presented by AASHTO [18], t_s has two main components, namely reaction time and braking time. The reaction time pertains to the human factors and denotes the time from the perception of the warning to the application of the break, during which the equipment continues travelling with its current speed and acceleration/deceleration. The research of reaction time is a long-standing trend for urban vehicles in traffic engineering [2,44,3]. For instance, Gazis et al. [20] and Wortman and Matthias [51] specify 1.14 s and 1.30 s, respectively, as the mean reaction time for an unalerted driver. The breaking time, on the other hand, is the time required for the equipment to come to a complete halt after the breaks are applied, during which time the speed of the equipment declines to zero from its current value. This component of t_s is more pertinent to the mechanics of the equipment and road conditions. Nevertheless, the research about the stoppage time is scarce for construction equipment where multiple DOFs should be considered. Guenther and Salow [22] suggested a value between 0.7 s to 1.5 s as a suitable stoppage time for mining excavation equipment. In another study, Stentz et al. [41] proposed a value between 2 s to 3 s as a value that is empirically found suitable for t_s for excavators. In this research, the value of t_s is considered to be 2 s.

In summary, the reviewed studies highlight the importance of considering the full scope of equipment related real-time information, including the pose, state and speed characteristics of the equipment, to generate the *DEW* considering the space limitations and the effective time window required to avoid potential collisions.

3. Proposed method

DEWs aim to use the pose, state, geometry, and speed characteristics of the equipment to generate a space around the equipment that would allow the prevention of immediate collisions with workers on-foot, other pieces of equipment or obstacles on site, considering t_s. Although according to the definition of t_s presented in Section 2.2, this value includes a period of moving with the current speed and a period of deceleration, in order to simplify the calculation process, this research conservatively assumes that the equipment continues to travel with its current speed and acceleration. Another assumption of the proposed method is that all pieces of equipment are equipped with an *RTLS* so that their poses and states can be calculated accurately. The update rate of *DEWs* is equal to the update rate of the corrected pose data (dt) coming from the *RTLS* used in the equipment. A rule-based system is used to identify the states of different equipment with a high accuracy by leveraging a set of equipment proximity and motion rules that determine the states of the equipment [47]. Also, a robust optimization-based method that uses geometric and operational characteristics of the equipment is used to improve the quality of the pose estimation (Vahdatikhaki et al., 2015).

Furthermore, in addition to the *DEWs* of equipment, workers on-foot and semi-dynamic obstacles (e.g., temporary structures),

also need to be tracked by means of RTLS and to be represented by their own corresponding safety zones to enable effective collision avoidance.

In this research, two types of equipment, namely excavators and trucks, are used as the main types of equipment that are typically used in earthwork operations. Excavators represent equipment that has articulated mechanism with rotational DOFs, whereas other types of equipment, e.g., trucks and rollers, are represented by trucks. However, at the abstract level of the discussion, *DEWs* of excavators are used as an example because they are more complicated than those of trucks due to their large number of DOFs.

Fig. 2 shows instances of a workspace that, unlike the *DEWs* shown in Fig. 1, consider the pose, state, geometry, and speed characteristics of the equipment. In such a workspace, depending on the state of the excavator, different shapes are used. Fig. 2(a) shows the *DEW* of an excavator in the swinging state that uses the magnitude of the rotation speed to determine the angle (α). However, ignoring the moving direction of the equipment may result in an uneconomic usage of the space that can be very valuable in a congested site. Therefore, it is recommended to consider the swinging direction of the equipment to differentiate between parts of the space to which the equipment is approaching and parts from which it is moving away. Fig. 2(b) shows the proposed workspace of an excavator in the swinging state where the direction of rotation is considered to differentiate between the angles of workspace on the rotation direction (α) and the opposite direction (β). The rationale behind the asymmetric shape of the workspace is that the risk of collision along the direction of movement is much greater than along the opposite direction. Thus, a greater accent should be placed upon the space at the moving direction of the equipment. This research proposes asymmetric workspaces that consider the moving direction of a piece of equipment in each state as explained in the following sections. This arrangement better captures the potentially hazardous space around the equipment while using the space frugally, rendering this type of workspace very suitable for congested sites.

For the DEWs to be effectively used for the purpose of collision detection and avoidance, every piece of equipment needs to be able to generate its own DEW and have near-real-time information about the DEWs of other equipment and the workers' workspaces. Fig. 3(a) shows the sequence diagram [4] of the communication between different pieces of equipment that enables the near-real-time exchange of DEWs and the subsequent collision detection. To avoid redundant computation, the equipment can perform pairwise comparisons only with the pieces of equipment that are in its vicinity. To determine the equipment in vicinity, the multi-layer workspace concept [7] (Luo et al., 2014) [29] can be applied. In this method the distance between every two pieces of equipment is calculated and if the distance is less than a specific threshold, then the collision detection between their DEWs is performed. In order to further reduce the computation efforts and avoid redundant calculations, the priorities of the different equipment can be used to delegate the calculation to the equipment with the lower priority. If a collision is detected between two pieces of equipment, the equipment with the lower priority will stop and send a warning to the other equipment. If both pieces of equipment have the same priority, then both should perform the collision detection and if a collision is detected they should both stop.

Similarly, Fig. 3(b) shows the sequence diagram of the communication between a piece of equipment and a worker on-foot. It should be clarified that given the workers vulnerability, they always have a higher priority over the equipment. As shown in Fig. 3(b), every piece of equipment receives the location of the worker and checks for the potential collision between its DEW and the cylindrical workspace of the worker. If a collision is

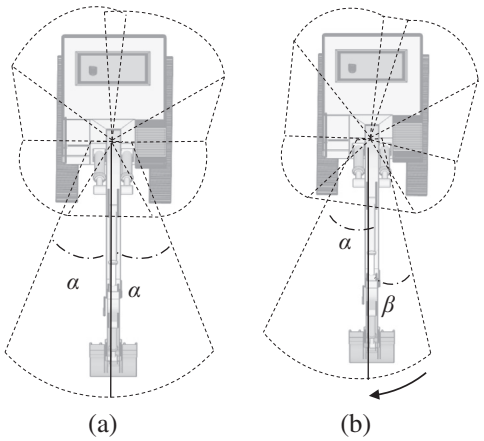

Fig. 2. (a) Symmetric workspace, and (b) proposed workspace.

detected, the equipment stops and sends a warning to the workers to clear out the dangerous zone. While it is indispensable to account for workers on-foot in addition to the equipment and semi-dynamic structures for effective collision avoidance on a construction site, the current paper focuses only on the collision between equipment. This is because, given the size of the equipment and their inherently more complex kinematics, the interaction between equipment is more complex and more difficult to monitor. Nevertheless, the proposed method can be easily applied to consider the workers as simple cylindrical workspace to avoid all types of collisions on a site.

Fig. 4(a) and (b) shows the flowchart for the generation of the proposed *DEWs* for excavator and trucks. In both flowcharts, with the 3D model of the equipment and its pose and state information available, the method proceeds to determine the linear and angular speeds of the equipment. For instance, as shown in Fig. 5(a), an excavator can travel on its tracks with the linear speed of $\vec{v}$, move its bucket with the linear speed of $\vec{v}_b$, or swing with the angular speed of $\vec{\omega}_1$. Fig. 5(b) shows the speeds corresponding to the controllable DOFs of a truck. The calculation of different speed and acceleration elements of the equipment is based on considering the changes in the pose of the equipment over two consecutive pose estimation data. The authors have previously showed how the pose estimation method can be used to accurately determine the 3D pose of the equipment, which includes the corrected location of the equipment and the orientation of the multiple parts of the equipment [48]. The linear speed elements can be calculated using the difference in the equipment location data over the time between two updates of the pose data (dt). Similarly, the angular speed can be calculated using the difference in the orientations of the different parts of the equipment over dt. The relevant acceleration elements can also be derived from these speed elements.

It should be emphasized that the pose estimation method applies the required corrections to the location data to remove the RTLS error up to an acceptable level (e.g., 20 cm) [48], but there is always a certain degree of residual error in the estimated pose that will propagate through the speed and acceleration calculation. However, as long as the amount of the residual error is within the acceptable level, the calculated speed and acceleration elements are considered reliable.

Upon the determination of the speed vectors, the *DEW* can be generated based on the type of the equipment and the equipment state as explained in the following sections. It should be emphasized that this method determines the shape of *DEWs* based on the assumption that the equipment is going to remain in its

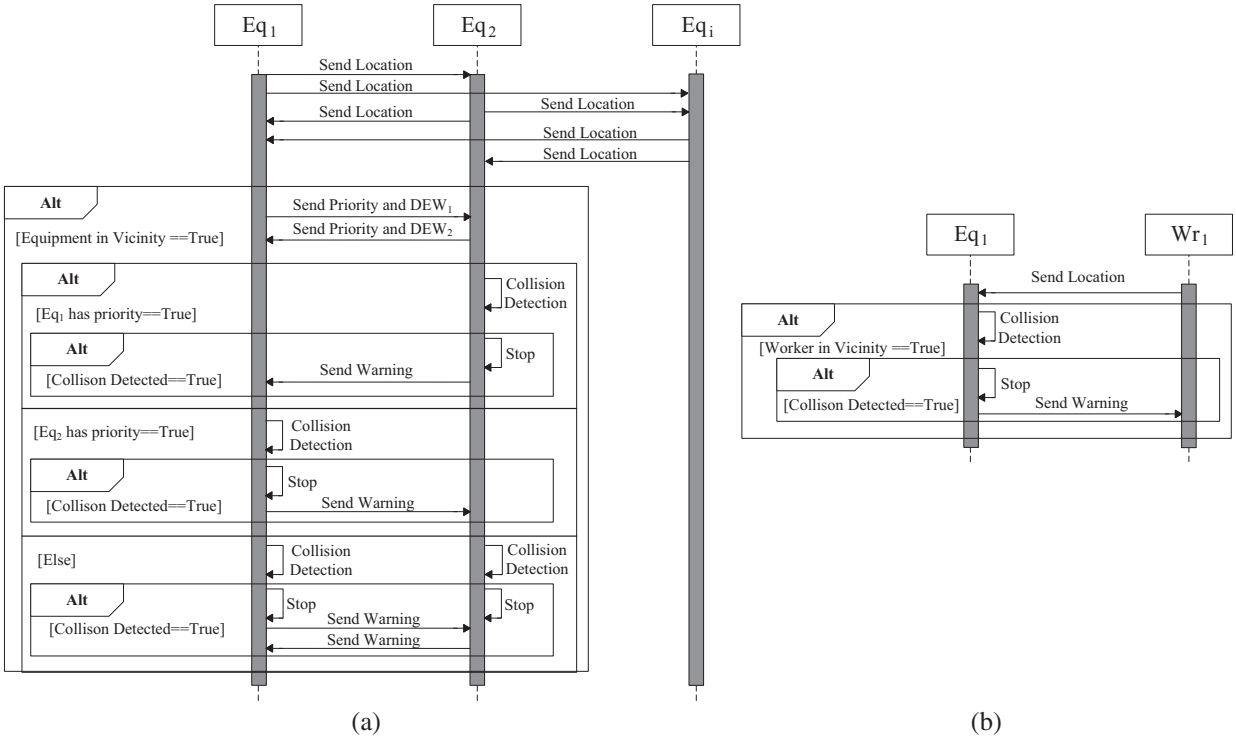

Fig. 3. Sequence diagram of communication between (a) several pieces of equipment, and (b) a piece of equipment and a worker using DEWs for safety control.

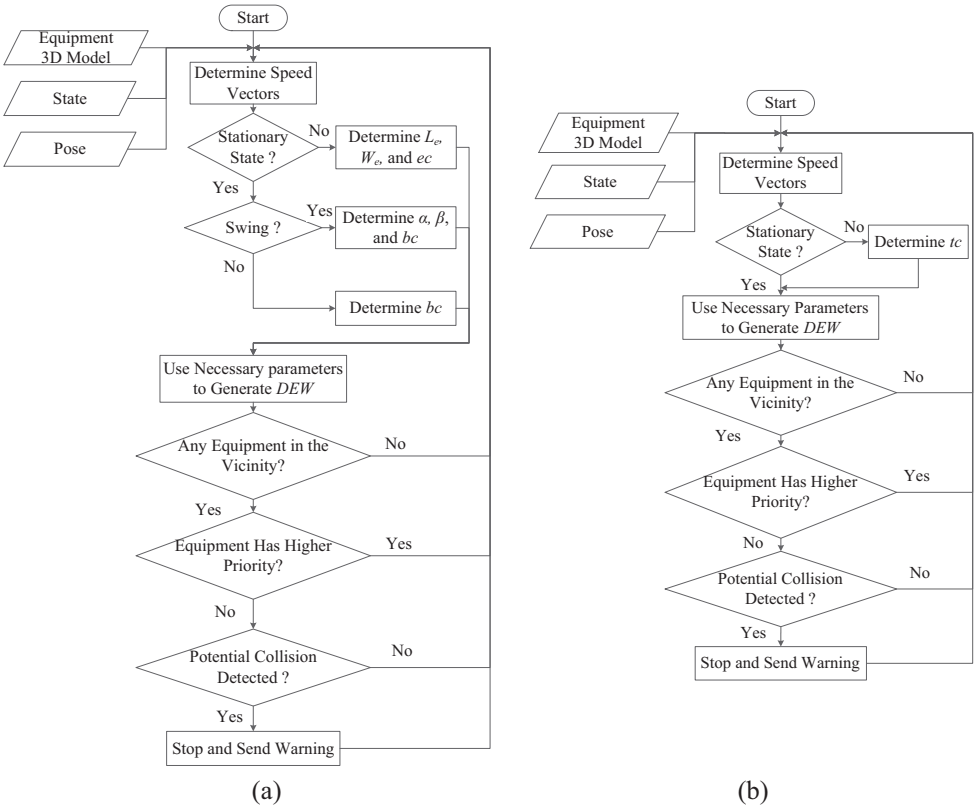

Fig. 4. Flowchart of the generation of DEW for (a) excavator, and (b) truck.

present state. Accordingly, the boundary situations, where the equipment is transiting between one state to another are not considered. However, this is tolerable in view of the high update rate of the *DEW*s. The types of the *DEW*s and the parameters that determine their shape are introduced in the following sections. Then, as explained above, the equipment with the lower priority (or both

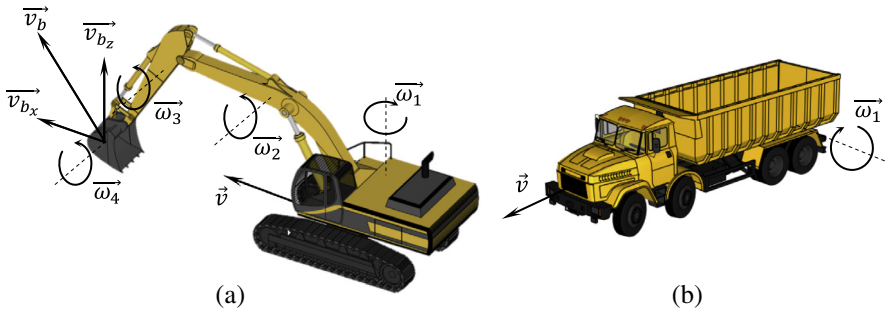

Fig. 5. Speed vectors corresponding to controllable DOFs for (a) an excavator, and (b) a truck (models of truck and excavator are obtained from Google 3D Warehouse [21]).

pieces of equipment if they have similar priorities) applies the collisions detection between *DEW*s of equipment in the neighborhood. If the collision is detected, warning is sent to the operators of the involved equipment with a lower or similar priority to stop.

It is also noteworthy that the generation of *DEWs* can be simplified by first calculating its projected shape in the *x*–*y* plane and then extruding it along the vertical axis so that the entire range of movement of the DOFs along the vertical axis is covered. However, a full 3D *DEW* will be investigated in the future.

3.1. DEW of excavators

Two distinct types of states can be identified for an excavator, namely stationary states (swinging, loading, dumping, and waiting) and traversal states (relocating, maneuvering). Usually an excavator can only engage in one of the two types at a time.

As shown in Fig. 5(a), a typical excavator can be controlled through five controllable DOFs resulting in the speed vectors $\overrightarrow{\omega_1}$, $\overrightarrow{\omega_2}$, $\overrightarrow{\omega_3}$, $\overrightarrow{\omega_4}$, and $\vec{v}$. However, since the workspace calculation is done in the *x*–*y* plane, three of the above-mentioned DOFs ($\overrightarrow{\omega_2}$, $\overrightarrow{\omega_3}$, $\overrightarrow{\omega_4}$) can be combined at any point in time to generate the instantaneous linear speed vector at the tip of the bucket ($\overrightarrow{v_b}$). This reduces the number of the speed vectors to three ($\overrightarrow{\omega_1}$, $\vec{v}$, $\overrightarrow{v_b}$).

3.1.1. DEW of excavator in stationary states

When an excavator performs stationary operations, it only moves along either or both of $\overrightarrow{\omega_1}$ and $\overrightarrow{v_b}$. This is because a skillful operator is able to control multiple DOFs along $\overrightarrow{v_b}$ while swinging. The shape of the DEW is defined based on the identified current stationary state of the excavator (swinging, loading, dumping, and waiting). Additionally, since the tracks of the excavator are not moving during the stationary states, *DEW* is defined only for the upper body of the excavator in these states.

(1) Excavator in swinging state: As shown in Fig. 6, if an excavator is identified to be in the swinging state with the angular speed of $\overrightarrow{\omega_1}$ and the linear speed of $\overrightarrow{v_b}$, the *DEW* is determined by the corresponding values of α, β and $\overrightarrow{v_{b_x}}$,where α represents the angle along the direction of rotation, β represents the angle in the opposite direction that is reserved for the possible change of swinging direction instigated by unforeseen circumstances, and $\overrightarrow{v_{b_x}}$ accounts for the combined movements of the boom, stick, and bucket in the vertical plane containing the axes of the boom and the stick.

For the simplicity of the calculation, each part of the equipment can be represented by a tight-fitting bounding box, as shown in Fig. 6(a). The *DEW* can be generated through the determination of the rotation radius for each bounding box (R_1, R_2, R_3, R_4, R_5), a buffer (b), t_s, the rotation angles α and β, and the bucket motion clearance (bc), as shown in Fig. 6(b).

R_1 is a variable that is defined as the distance from the excavator's center of rotation to the furthest point on the boom, stick, and bucket axis in the *x*–*y* plane at the current time. R_2 to R_5 are fixed parameters that are dictated by the equipment geometry and correspond to the distances from the excavator's center of rotation to the front and rear corners of the upper body of the excavator. b is also a fixed parameter used in order to define *DEW* with a degree of conservativeness. b is proportionate to the size of equipment and can be defined as a percentage of the maximum dimension of the equipment, for example 1% of the length of the equipment, and is applied along the radii R_i. Other factors that may have impact on the value of b are the update rate and the accuracy of the applied RTLS. Another buffer (b) is added to the bounding box that contains the boom, stick and the bucket, as shown in Fig. 6(b).

The angle β represents the amount of swing the excavator will do over t_s if the operator stops the swinging in its current direction and swings in the opposite direction for any reasons. With this definition, β is a function of ω_1, t_s, and the swinging acceleration/deceleration (τ_s), assuming that they are equal. τ_s is a predefined value due to the fact that it pertains to the acceleration and deceleration that are expected to happen in case of swing direction shift. Eq. (1) can be derived from basic kinematic equations [19] for the calculation of β.

$$\beta = \frac{1}{2}\tau_s\left(t_s - \frac{\omega_1}{\tau_s}\right)^2 - \frac{{\omega_1}^2}{2\tau_s} \tag{1}$$

The angle α, on the other hand, denotes the amount of swing the excavator will be doing in the current direction provided it continues with its current speed ($\overrightarrow{\omega_1}$) and acceleration/deceleration (τ_a). Unlike τ_s, τ_a is a value measured in real time because it considers the current actual acceleration. Nevertheless, τ_a will be zero during most of the swinging operation since most excavators tend to reach to the steady state swinging speed quickly and then continue with that speed. Similarly, when the swinging is completed, the excavator decelerates to a complete halt quickly. Based on this definition, α is a function of τ_s, ω_1, and t_s, as shown in Eq. (2).

$$\alpha = \frac{1}{2}\tau_a \times t_s^2 + \omega_1 \times t_s \tag{2}$$

bc represents the clearance buffer for the movement of the bucket along the boom, stick, and bucket axis when the skilled operator is combining the swinging motion with boom/stick/bucket movement away from the excavator [38]. It is determined by $\overrightarrow{v_{b_x}}$ (the projection of $\overrightarrow{v_b}$ on the horizontal plane), its corresponding measured acceleration (τ_{b_x}), and t_s, as given in Eq. (3). To generate *DEW* conservatively, bc is defined based only on the outward tilting of the combination of bucket/stick/boom movement and it ignores the inward tilting.

$$bc = \frac{1}{2}\tau_{b_x} \times t_s^2 + v_{b_x} \times t_s \tag{3}$$

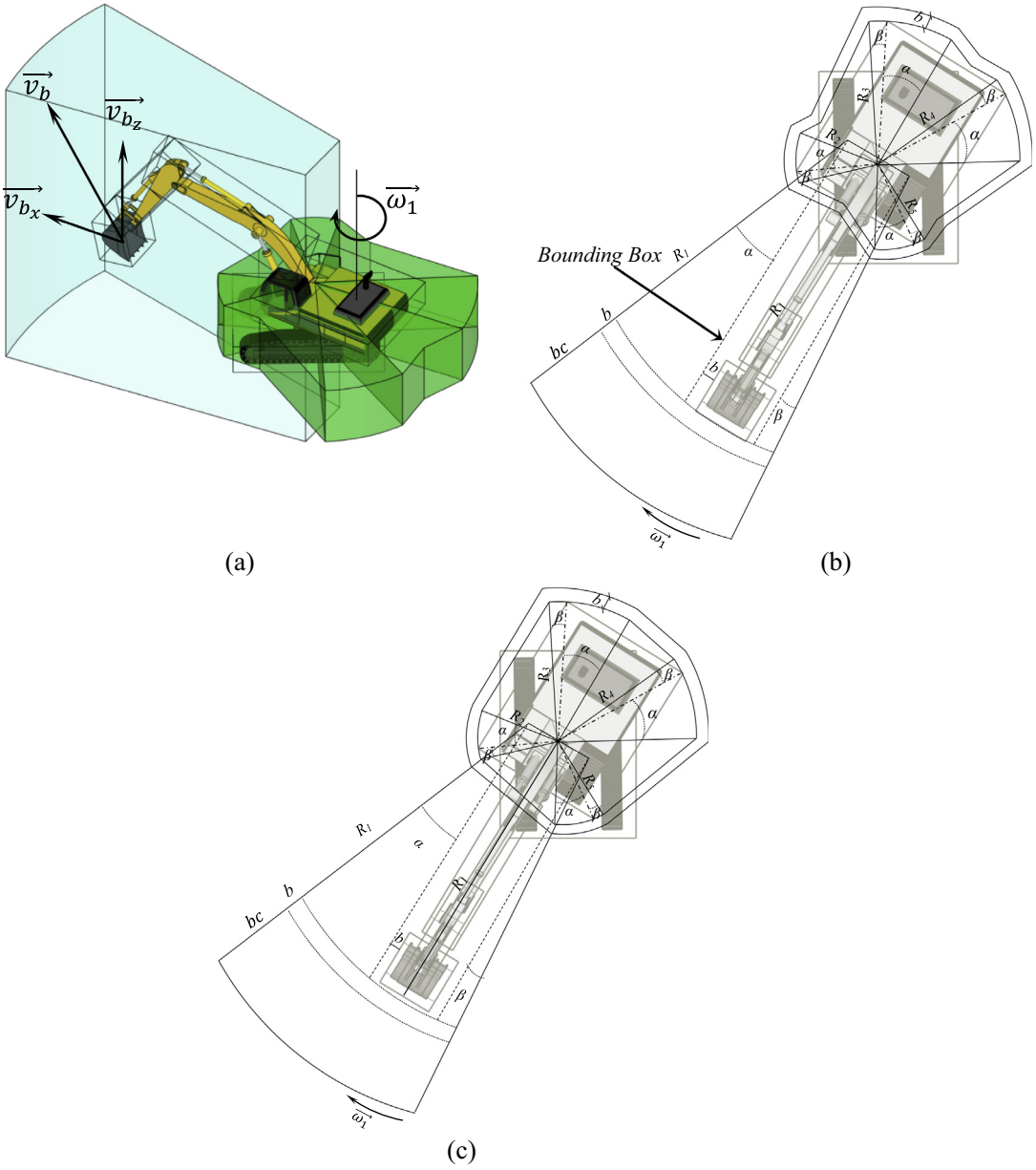

Fig. 6. Schematic (a) 2D and (b) 3D and (c) simplified 2D representations of DEW of an excavator in swinging state.

Although the accurate representation of the *DEW* for the swinging state is as shown in Fig. 6(a) and (b), a conservative simplification can be made to the geometry of the *DEW* by connecting the corners of the pie shapes resulting from the rotations of each corner of the bounding boxes, as shown in Fig. 6(c).

(2) Excavator in loading/dumping states: Fig. 7 shows the workspace when the excavator is in the loading/dumping states. Since the excavator's upper body is not swinging in these states, it is enough to reserve space for the movement of the boom/stick/bucket using a buffer. The shape presented in Fig. 7 is the natural result of the excavator workspace in the swinging state, shown in Fig. 6(c), when ω_1 and τ_s are zero, and thus α and β are zero. Accordingly, the workspace in these states is determined mainly by *b* and *bc*, where the calculation of *bc* is done similar to the case of the swinging state through Eq. (3).

(3) Excavators in waiting state: The excavator workspace during the waiting state resembles that of Fig. 7, with the difference that since the excavator is not engaged in any operations, the value of *bc* is zero.

3.1.2. DEW of excavator in traversal states

Whereas Figs. 6 and 7 illustrate the basic principle behind the generation of *DEW* for an excavator in stationary states, Fig. 8 depicts the ruling parameters in forming the *DEW* when the excavator is performing traversal operations (i.e., relocating or maneuvering along $\vec{v}$). The workspace in this case is a box whose dimensions are regulated by (1) the dimensions of a bounding box representing the entire excavator (L_e, W_e) at a given pose, where L_e and W_e are the instantaneous length and width of the equipment, a buffer (b), and the excavator motion clearance (ec). Unlike the workspace in stationary states, where the tracks were disregarded from the *DEW*, in traversal states, the tracks need be incorporated in the workspace. This is because the tracks are not stationary and can be a source of collision risks. Given that the *DEW* is an instantaneous workspace generated solely based on the pose and the speed characteristics of the equipment, it is defined linearly along $\vec{v}$, even if the equipment is actually moving on a curved path. However, if the construction site has a road network, then the location data of the equipment can be integrated

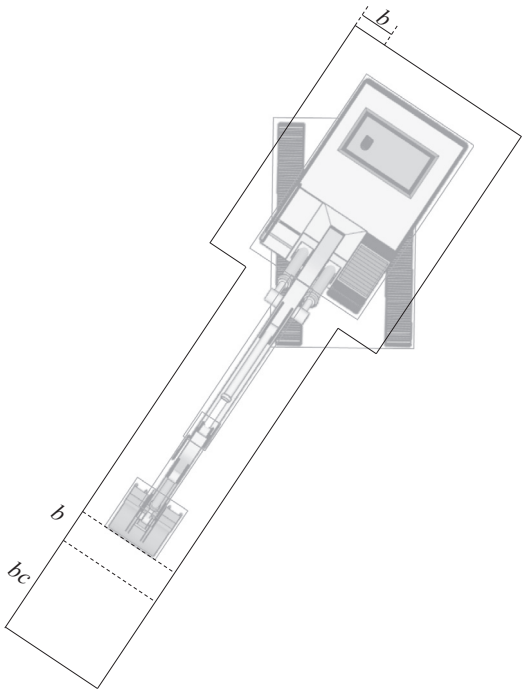

Fig. 7. Schematic representation of DEW of an excavator in loading and dumping states.

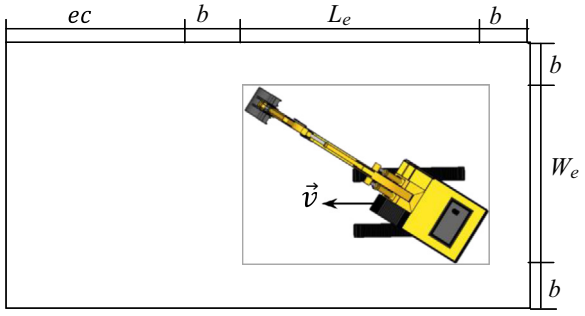

Fig. 8. Schematic representation of DEW of an excavator in traversal states.

with the road data to ensure that the workspace is following the road alignment. This integration is not currently considered in this research but will be addressed in the future.

The rationale behind b is similar to the one explained earlier in Section 3.1.1. ec represents the clearance buffer for the movement of the excavator when it moves on its tracks along the speed vector $\vec{v}$. It is therefore a function of v, measured τ_t, and t_s as given in Eq. (4).

$$ec = \frac{1}{2}\tau_t \times t_s^2 + v \times t_s \tag{4}$$

3.2. DEW of trucks

Similar to excavators, truck can be also engaged in two distinct types of states, namely stationary states (loading, dumping, and waiting.) and traversal states (hauling, returning, and maneuvering).

3.2.1. DEW of truck in stationary states

The stationary states for the truck are loading, dumping and waiting. Due to the simple geometry of trucks, the *DEW* for the truck is basically represented by a box whose dimensions follow the dimensions of the equipment (L_t, W_t) with an additional buffer (b_t). Fig. 9(a) represents the *DEW* for the truck in stationary states. Note that in the dumping state, an additional buffer should be added to the rear of the truck based on the speed at which the material is being spread, which is a function of the type of soil and the rotating angle of the bed of the truck. However, the present paper does not cover the details of this case.

3.2.2. DEW of truck in traversal states

The truck is in a traversal state when it is hauling the material to the dumping area, returning to the excavation area, or maneuvering at the loading or dumping areas. The *DEW* of a truck in these states is determined by the equipment dimensions (L_t, W_t), a buffer (b_t) and a truck motion clearance (tc). tc is calculated using an equation similar to Eq. (4). Fig. 9(b) represents the *DEW* for the truck in traversal states. It should be noted that when the truck is maneuvering, it may be moving backward. In such scenarios, tc is applied at the rear of the equipment.

Once the *DEWs* of all pieces of equipment are generated, it is possible to identify the potential conflicts between them and take the required corrective measures, e.g., alerting the operator or stopping the equipment.

3.3. An example of the application of DEW

Fig. 10 shows a scenario in which a truck enters a site, maneuvers to the loading area where an excavator is digging a trench, gets loaded by the excavator and departs from the site. As shown in Fig. 10, the orientation and size of the truck's *DEW* change according to its varying direction and magnitude of its speed vectors ($\vec{v}_i$), respectively. It is worth mentioning that not all types of collisions among workspaces and safety zones are actually a safety threat. For instance, as shown in Fig. 10, while the collision between the workspaces of the truck and the excavator may lead to a safety hazard, an overlap between their workspaces is inevitable as part of the regular excavation work cycle. This limitation is because of the simplified shape of *DEW* along the vertical axis resulting in seemingly overlapping workspaces. However, in future a full 3D *DEW* that accounts for the geometry and kinematics of excavators along the vertical axis will be developed to address this shortcoming.

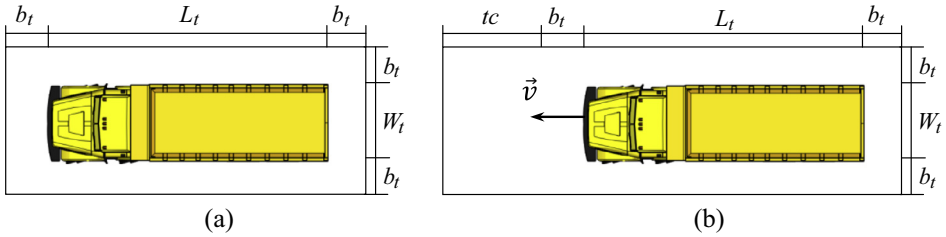

Fig. 9. Schematic representations of DEW of a truck in (a) stationary states, and (b) traversal states.

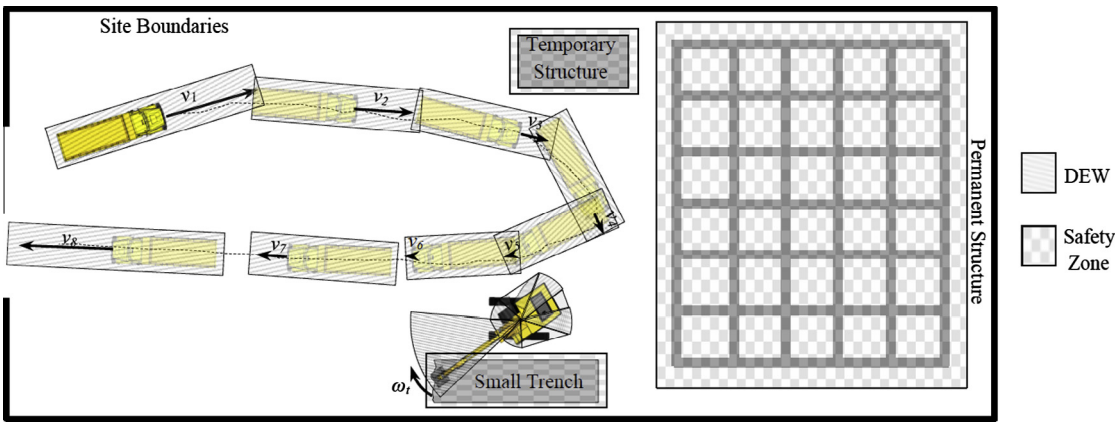

Fig. 10. Schematic representation of safety analysis based on DEWs.

3.4. Analysis of congestion level

In addition to benefiting the safety of site by preempting the potential collisions between different pieces of equipment, *DEWs* can also serve to calculate an index of the congestion level on the site in preparing site reports. Two approaches are presented in the literature for the quantification of congestion level on the site. Dawood and Mallasti [16] calculated the congestion level through an index named space criticality, which is the result of dividing the summation of *DEWs* sizes by the size of the site. Nevertheless, this index does not capture the temporal aspect of the used space. In another approached proposed by Andayesh and Sadeghpour [1], the congestion level is represented through the space requirement index, which is the result of the summation of the multiplication of *DEWs* sizes by their corresponding durations. Unlike the previous approach, this approach ignores the volume of the site. Therefore, in this research it is proposed to integrate the two approaches to capture both the temporal dimension of the *DEWs* and the space availability, i.e., the size of the site. For this purpose, if a precise record of *DEWs* for different pieces of equipment and the number of hours they have been working on the site are available, the multiplication of the average volume of *DEW* (V_i) and the equipment working hours (H_i) would indicate how much space the equipment required to perform its work over its working hours. The summation of these values for all the equipment divided by the multiplication of the site area (A_s) and the overall working hours for which the congestion is being calculated (H_0) would present an index that indicates how much space has been used on the site and for how long. The congestion index (CI) can be calculated as shown in Eq. (5). The greater the congestion index, the more space has been used over the analysis duration.

$$\mathrm{CI} = \frac{\sum_{i=1}^{n} H_i \times V_i}{A_s \times H_0} \tag{5}$$

where n is the number of equipment.

4. Implementation and case study

A case study was conducted to verify and validate the proposed method for generating *DEWs*. The data from a previously conducted lab test [47] were used to demonstrate the generation of *DEW* and its ability to effectively preempt potential collisions between equipment. As shown in Fig. 11, three pieces of remotely controlled scaled equipment were employed to simulate an earthwork operation where an excavator is dumping a hypothetical load to a dump truck, which in turn hauls the material to a dumping zone, dumps it, and then returns to the loading spot for the next load.

Ubisense's Ultra Wideband (UWB) technology [46] was used to track the equipment. State and pose identification methods proposed in the authors' previous works (Vahdatikhaki et al., 2015)

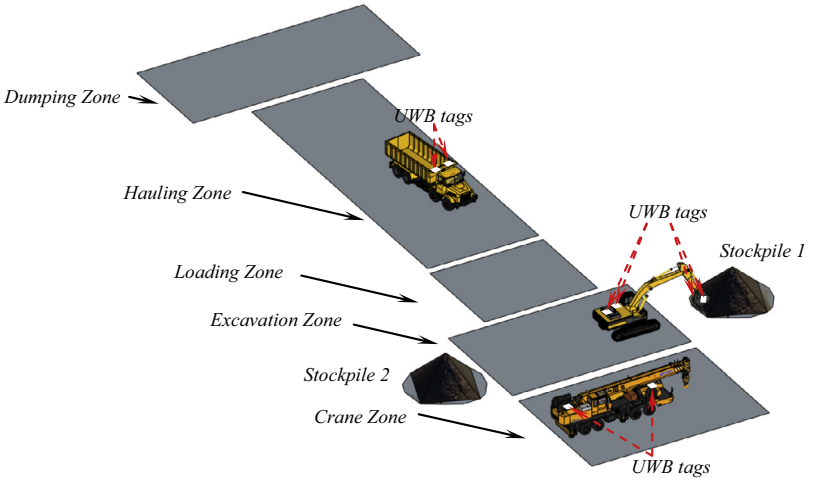

Fig. 11. Schematic layout of simulated site in the case study.

[48] have been deployed to provide the required input data. The update rate of the corrected pose base on the UWB data (dt) is 1 Hz.

In the simulated operation, three pieces of remotely controlled scaled equipment were used to replicate a typical earthmoving operation. The number and location of tags attached to different pieces of equipment are shown in Fig. 11. As shown in this figure, in this operation, the truck travels from the dumping zone to the loading zone, get loaded by the excavator, and then hauls the material to the dumping zone. This cycle was repeated four times. The excavator, on the other hand, obtains a load from the stockpile and dumps it on the truck when the truck is waiting in the loading zone. During the first two cycles, the excavator worked near the stockpile 1 and then relocated to the other side of the excavation zone to work near the stockpile 2 for the next two cycles of the operation. With the intention to create a congested site, a crane was placed near the excavator without actively engaging in the simulated operation. Also, upon the completion of the fourth loading cycle, the excavator was intentionally steered to collide with the crane, to evaluate the effectiveness of *DEW* in preempting the potential collision.

The proposed method for the generation of *DEWs* was implemented using Microsoft Excel. The implementation at the present stage does not incorporate the equipment communication structure explained in Section 3, and generates the DEWs and controls the collisions using a centralized method, where the central platform performs all the computations. The recorded UWB coordinates, the corrected pose, and the states of different pieces of equipment are imported into an Excel sheet as the input. The governing equations that generate *DEWs* were developed in Excel, as explained in Section 3.1. At every time step, the relevant speeds and accelerations/decelerations of the equipment are measured, and the corresponding *DEW* is generated. For the collision detection between DEWs, an automated method was used based on the line segment intersection algorithm [17]. In this method, all edges of the two DEWs are checked against one another for potential intersection using many-to-many relationship. The arc part of the DEW is approximated by two segments. *A* collision is detected when a pair of edges is found intersecting. In this case study, which was implemented using a personal computer with an Intel Core i7-2600 CPU (3.40 GHz), the calculation time for the generation of the *DEW*s and the collision detection were measured. The average calculation time and its standard deviation were found to be 23.10 ms and 1.2 ms, respectively.

In the generation of *DEW*, the values of t_s, b, *and* τ_s were set to 2 s, 5 cm, and 2 $\frac{deg}{s^2}$, respectively. The parameters used for different pieces of equipment are shown in Table 1.

Fig. 12 illustrates several snapshots of the generated *DEWs* at different stages of the simulated operation. Fig. 12(a) shows the equipment at the inception of the operation. The locations of attached tags on the equipment are indicated by the cross symbols. The *DEW*s of different pieces of equipment are shown using the dotted lines surrounding the equipment. The front of the truck is distinguished by the locations of the tags attached to the front of the bed.

Fig. 12(b) shows the hauling truck and its corresponding *DEW*. The length of the *DEW* ahead of the truck is determined by the instantaneous speed of the truck at that point in time. Fig. 12(c) depicts the excavator at the beginning of the swinging state. The excavator *DEW* in the relocation state is shown in Fig. 12(d). Fig. 12(e) shows a part of the operation when the truck was moving backward to adjust itself for loading. In this case, the extension of the *DEW* takes place at the rear of the equipment, representing the potential area of collision. Finally, Fig. 12(f) shows the last phase of the operation where the excavator was intentionally steered towards a collision with the crane. As shown in this figure, the *DEWs* could be used to successfully identify and warning against the impending collision 4 s before the actual collision.

In order to demonstrate the effectiveness of the *DEWs*, a comparison was made between the proposed method and the alternative types of workspaces shown in Figs. 1 and 2. The R for the cylindrical workspace and b for the buffer workspace were set to 50 cm and 5 cm, respectively. Table 2 shows the results of the comparison, where different methods were analyzed in terms of the average size (the area reserved by the generated workspace in different states), the number of triggered warnings, the number of false warnings (false positive), the number of missed warnings (false negative), and the average time between the warning and the actual collision (collision detection clearance time).

The workspace area is measured in terms of the averaged area and its standard deviation, based on the simplification that the height is the same for all the workspaces. The space saving was calculated through comparing the averaged areas of every method with the area of cylindrical workspace, which is the worst case in terms of the space economy. Regarding the number of warned collisions, the values represent the number of instances (out of the total 366) where the collision between two workspaces generated

Table 1
List of different parameters used for the generation of DEW.

Excavator-swing

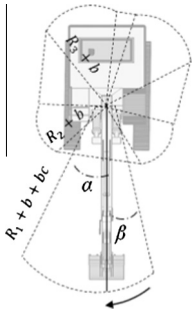

Parameter	Value
R_1	Variable
R_2, R_4	20 cm
R_3, R_5	25 cm

Excavator-relocation

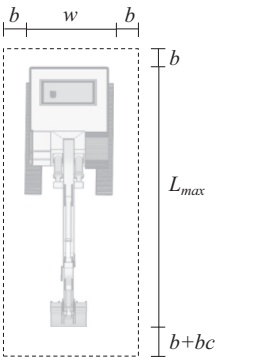

Parameter	Value
w	20 cm
L_{max}	68 cm

Truck-traversal state

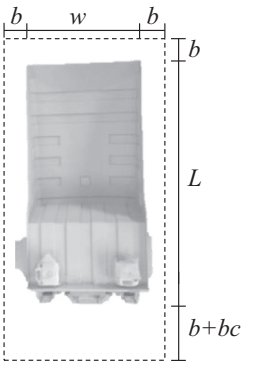

Parameter	Value
w	20 cm
L	42 cm

Crane-stationary state

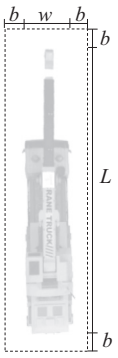

Parameter	Value
w	14 cm
L	91 cm

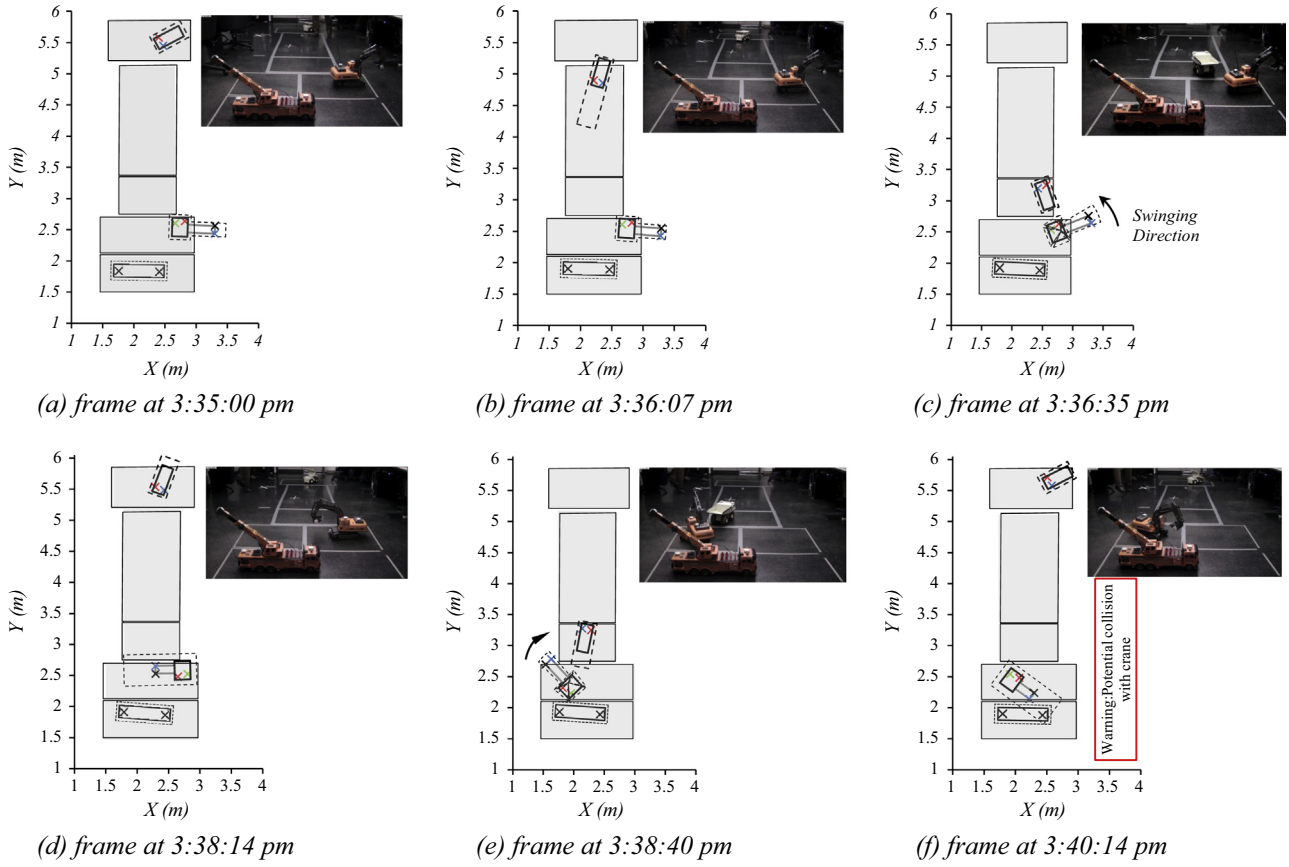

Fig. 12. Results of generated DEWs of the case study.

Table 2
Comparison of different types of workspaces.

Parameter	Method			
	Proposed workspace	Symmetric workspace	Buffer workspace	Cylindrical workspace
Swing workspace area [μ and σ] (m^2)	[0.22, 0.03]	[0.25, 0.06]	N/A	N/A
Loading/dumping workspace area [μ and σ] (m^2)	[0.24, 0.02]	[0.24, 0.02]	N/A	N/A
Relocation workspace area [μ and σ] (m^2)	[0.49, 0.06]	[0.49, 0.06]	N/A	N/A
Overall averaged workspace area [μ] (m^2)	0.25	0.27	0.22	0.78
Space savings (compared to cylindrical workspace) (%)	67.95	65.38	71.80	0
False positive warnings (%)	24.53	25.00	29.24	68.81
False negative warnings (%)	0	0	0	0
Collision detection clearance time [μ and σ] (s)	[4.28, 1.16]	[4.43, 1.05]	[3.28, 1.58]	[5.0, 0]

warnings. A collision is defined as any instances where the distance between the pair of equipment was less than 5 cm. The false positive warning is defined as any warnings that did not entail actual collisions within the next 5 s. The false negative warning, on the other hand, is the count of unwarned collisions. Finally, the collision detection clearance time is computed by finding the earliest warnings prior to a collision.

It can be discerned that the proposed workspace takes less space than the symmetric workspace, with the space saving of 67.95%, and the least false positive, i.e., 24.53%, which represents the reliability of the workspace. Another interesting observation is that both the proposed and the symmetric workspaces perform efficiently by successfully warning against every collision within the average of more than 4 s, only 1 s less than the best case that belongs to the cylindrical workspace. In the observed clearance times, no instance with a clearance time less than the stoppage time was recorded for the proposed, symmetric and cylindrical workspaces. Only in the case of the buffer workspace, one instance with the clearance time of 1 s was observed. Therefore, the proposed workspace always provided enough clearance for collision avoidance.

While the cylindrical workspace provides the best collision detection clearance, it occupies more than 3 times space than that of the proposed workspace and tends to trigger a considerable number of false warnings. The buffer workspace outperforms other types of workspaces in terms of the space economy, but has the least clearance time. Although the improvement of the space saving in the proposed workspace is not significantly more than the symmetric workspace, the difference is determined mainly by the length of the stoppage time. In this case study, the stoppage time was set at 2 s, but should the stoppage time be increased, the difference in the space saving is expected to rise noticeably.

In all types of workspaces, no false negative is observed. This phenomenon can be explained in the view of the nature of the

Table 3
Values used for the calculation of the congestion index.

Parameter	Equipment		
	Excavator	Truck	Crane
Working hours (hour)	0.10	0.10	0.10
Average volume of *DEW* (m^3)	0.125	0.053	0.162
Overall occupied space ($m^3 \times$ hour)	0.013	0.005	0.016

workspaces, which is to create a safety buffer around the equipment. As such, the collision between workspaces always happens prior to the actual collision. However, false negatives can happen if the communication network between the equipment is disrupted or the update rate of the corrected pose data is less than the stoppage time. In the case study, none of these cases happened, and the proposed method assumes that the robust infrastructure is available for the generation of *DEW*s.

Given that the operation took nearly 6 min, the overall area of the site was 18 m^2, and all pieces of the equipment have been present on the site during this time, the required data for the calculation of the congestion index can be collected as shown in Table 3. Using Eq. (5), the overall space usage and the congestion index are calculated as 0.034 ($m^3 \times$ hours) and 0.019 ($\frac{m^3 \times hours}{m^2 \times hours}$), respectively.

Although the presented case study is a good indication of the efficiency of the proposed method in terms of reducing the number of false alarms and more effective use of space compared to other types of the existing workspaces, the scale of the equipment used in the case study posed some limitations. First, the effect of the residual error on the accurate pose estimation of the scaled equipment is relatively larger than the case of the actual equipment, due to the small size of the equipment. Second, although it was tried to introduce some noise to the UWB tracking system in the laboratory by partially obstructing the direct line of sight between sensors and tags, there is a need to test the tracking system under the conditions of actual construction sites. However, applying such a test will require careful considerations of some technical and logistical difficulties that might influence the performance of the UWB system, including the proper calibration of the UWB system under the pressure of the actual construction work, the setting of the UWB cables, and the smooth collaboration with the contractors.

5. Discussion

The main contribution of the presented method for the generation of *DEW*s is the use of equipment's state, speed, geometry and pose data to economically mark the safety workspace around different pieces of equipment. It is shown in the case study that the proposed method is capable of warning against all potentially hazardous proximity without using the space over-conservatively or generating too many false alarms. Nevertheless, there is a positive correlation between the level of congestion and the rate of false positive alarms generated by the DEWs. However, this is coming from the nature of the problem rather than the characteristics of the proposed method. Although the rate of false positive rises with the increase in the congestion level, the rate would still remain lower than the rate of false positive alarms generated by the conventional methods, e.g., cylindrical workspace. Also, it should be highlighted that generally with the increase in the congestion level, the average speed by which the equipment travels on site will also decreases, resulting in a smaller average DEW area, which in turn results in a smaller chance of false alarms.

6. Conclusions and future work

This paper proposed a novel method for the generation of real-time dynamic equipment workspaces considering the pose, state, geometry, and the speed characteristics of the equipment. This method is built on the previous work of the authors, where robust methods for the calculation of pose and state of different pieces of equipment based on *RTLS* data were presented. The present method considers the required operator stoppage time to determine how much space needs to be reserved in order to ensure that the equipment will not collide with other pieces of equipment in the immediate future. Excavators and trucks were used as the representatives of different types of equipment used in an earthwork project. The appropriate *DEW*s and their calculation process for all possible states of the equipment were presented. Finally, the application of *DEW*s for the calculation of congestion index was discussed.

In view of the results of the case study, it can be concluded that: (1) the proposed method is providing a balance between economic use of space and the ability to warn against potential collisions in an effective manner using the pose, state, geometry, and speed characteristics of the equipment, (2) the flexibility of the method in using more than one speed vector in the calculation of *DEW*s enabled effective capturing of the operation of skilled operators where multiple DOFs can be used simultaneously.

Finally, some false warnings resulted from capturing the movement along various DOFs only in 2D. Therefore, the future efforts of the authors are dedicated to avoiding this problem by considering the details of the movement in the third dimension in the generation of *DEW*s. Also, the authors plan to conduct a test on a construction site where the UWB system can be tested under the actual site conditions.

Acknowledgments

This research has been supported by grants from the National Science and Engineering Research Council of Canada and Work Safe BC. This support is greatly appreciated.

References

[1] M. Andayesh, F. Sadeghpour, The time dimension in site layout planning, Automat. Constr. 44 (2014) 129–139.
[2] J.E. Baerwald, M.J. Huber, L.E. Keefer, Transportation and Traffic Engineering Handbook, third ed., Prentice Hall, Englewood Cliffs, New Jersey, 1965.
[3] W. Barfield, T.A. Dingus, Human Factors in Intelligent Transportation Systems, Lawrence Erlbaum Associates, Mahwah, New Jersey, 1998.
[4] G. Booch, J. Rumbaugh, I. Jacobson, The Unified Modeling Language User Guide, Addison-Wesley, Reading, PA, 1999.
[5] R.L. Burns, Dynamic Safety Envelope for Autonomous-Vehicle Collision Avoidance System, Patent No. US 6393362 (2002).
[6] A. Carbonari, A. Giretti, B. Naticchia, A proactive system for real-time safety management in construction sites, Automat. Constr. 20 (6) (2011) 686–698.
[7] S. Chae, Development of warning system for preventing collision accident on construction site, in: Proceedings of the 26th Int. Symposium on Automation and Robotics in Construction, 2009.
[8] S. Chae, T. Yoshida, Application of RFID technology to prevention of collision accident with heavy equipment, Automat. Constr. 19 (3) (2010) 368–374.
[9] R. Chavada, N.N. Dawood, M. Kassem, Construction workspace management: the development and application of a novel Nd planning approach and tool, ITcon 17 (2012) 213–236.
[10] T. Cheng, Automated Safety Analysis of Construction Site Activities Using Spatio-temporal Data, Doctoral Dissertation, Georgia Institute of Technology, 2013.
[11] T. Cheng, J. Teizer, Real-time resource location data collection and visualization technology for construction safety and activity monitoring applications, Automat. Constr. 34 (2013) 3–15.
[12] S. Chi, C.H. Caldas, Automated object identification using optical video cameras on construction sites, Comput.-Aided Civ. Infrastruct. Eng. 26 (5) (2011) 368–380.
[13] S. Choe, F. Leite, D. Seedah, C. Caldas, Evaluation of sensing technology for the prevention of backover accidents in construction work zones, J. Inf. Technol. Constr. 19 (2014) 1–19.
[14] CRC Mining, Shovel Load Assist Program, CRC Mining, 2013. <http://www.crcmining.com.au/breakthrough-solutions/shovel-load-assist-project/>.
[15] V.J. Davies, K. Tomasin, Construction Safety Handbook, Thomas Telford, 1996.
[16] N. Dawood, Z. Mallasi, Construction workspace planning: assignment and analysis utilizing 4D visualization technologies, Comput.-Aided Civ. Infrastruct. Eng. 21 (7) (2006) 498–513.

[17] M. De Berg, M. Van Kreveld, M. Overmars, O.C. Schwarzkopf, Computational Geometry, Springer, Berlin, Heidelberg, 2000.
[18] D.B. Fambro, K. Fitzpatrick, R.J. Koppa, Determination of Stopping Sight Distances, Transportation Research Board, 1997.
[19] J. Forshaw, G. Smith, Dynamics and Relativity, John Wiley & Sons, 2009.
[20] D. Gazis, R. Herman, A. Maradudin, The problem of the amber signal light in traffic flow, Oper. Res. 8 (1) (1960) 112–132.
[21] Google 3D Warehouse, 2014. <https://3dwarehouse.sketchup.com/?redirect>.
[22] N. Guenther, H. Salow, Collision avoidance and operator guidance innovating mine vehicle safety, in: Queensland Mining Industry Health & Safety Conference, Townsville, 2012.
[23] A. Hammad, C. Zhang, M. Al-Hussein, G. Cardinal, Equipment workspace analysis in infrastructure projects, Can. J. Civ. Eng. 34 (10) (2007) 1247–1256.
[24] J. Hinze, X. Huang, L. Terry, The nature of struck-by accidents, J. Constr. Eng. Manage. 131 (2) (2005) 262–268.
[25] J.W. Hinze, J. Teizer, Visibility-related fatalities related to construction equipment, Saf. Sci. 49 (5) (2011) 709–718.
[26] T. Howarth, P. Watson, Construction Safety Management, Wiley-Blackwell, 2009.
[27] R.B. Hukkeri, Machine Control System Implementing Intention Mapping, U.S., Patent No. US 2012/0130582 A1 (2012).
[28] C. Kim, C. Haas, K. Liapi, C. Caldas, Human-assisted obstacle avoidance system using 3D workspace modeling for construction equipment operation, J. Comput. Civ. Eng. 20 (3) (2006) 177–186.
[29] X. Luo, W.J. O'Brien, F. Leite, J.A. Goulet, Exploring approaches to improve the performance of autonomous monitoring with imperfect data in location-aware wireless sensor networks, Adv. Eng. Inform. 28 (4) (2014) 287–296.
[30] D.V. MacCollum, Construction Safety Planning, John Wiley & Sons, 1995.
[31] E.D. Marks, Active Safety Leading Indicators for Human–Equipment Interaction on Construction Sites, Doctoral Dissertation, Georgia Institute of Technology, 2014.
[32] E.D. Marks, J. Teizer, Method for testing proximity detection and alert technology for safe construction equipment operation, Constr. Manage. Econ. 31 (6) (2013) 636–646.
[33] Z. Mallasi, N. Dawood, Workspace competition: assignment, and quantification utilizing 4D visualization tools, Proc. Conf. Constr. Appl. Virtual Reality (2004) 13–22.
[34] M. McCann, Heavy equipment and truck-related deaths on excavation work sites, J. Saf. Res. 37 (5) (2006) 511–517.
[35] H. Moon, H. Kim, C. Kim, L. Kang, Development of a schedule-workspace interference management system simultaneously considering the overlap level of parallel schedules and workspaces, Automat. Constr. 39 (2013) 93–105.
[36] A. Oloufa, M. Ikeda, H. Oda, GPS-Based Wireless Collision Detection of Construction Equipment, NIST Special Publication sp, 2003, pp. 461–466.
[37] N. Pradhananga, Construction Site Safety Analysis for Human–Equipment Interaction using Spatio-Temporal Data, Doctoral Dissertation, Georgia Institute of Technology, 2014.
[38] P. Rowe, A. Stentz, Parameterized scripts for motion planning, in: Proceedings of the 1997 IEEE/RSJ International Conference on Intelligent Robots and Systems, IEEE, 1997, pp. 1119–1124.
[39] T. Ruff, Evaluation of a radar-based proximity warning system for off-highway dump trucks, Accident Anal. Prev. 38 (1) (2006) 92–98.
[40] SAFEmine, Advanced Traffic Safety Solution for Surface Mining, SAFEmining, 2014. <http://www.safe-mine.com/index.php/products#cas>.
[41] A. Stentz, J. Bares, S. Singh, P. Rowe, A robotic excavator for autonomous truck loading, Auton. Robots 7 (2) (1999) 175–186.
[42] S. Talmaki, V.R. Kamat, Real-time hybrid virtuality for prevention of excavation related utility strikes, J. Comput. Civ. Eng. 28 (3) (2014).
[43] K. Tantisevi, B. Akinci, Automated generation of workspace requirements of mobile crane operations to support conflict detection, Automat. Constr. 16 (3) (2007) 262–276.
[44] G.T. Taoka, Brake reaction times of unalerted drivers, ITE J. 59 (3) (1989) 19–21.
[45] J. Teizer, B.S. Allread, C.E. Fullerton, J. Hinze, Autonomous pro-active real-time construction worker and equipment operator proximity safety alert system, Automat. Constr. 19 (5) (2010) 630–640.
[46] Ubisense, 2013. <http://www.ubisense.net/en/>.
[47] F. Vahdatikhaki, A. Hammad, Framework for near real-time simulation of earthmoving projects using location tracking technologies, Automat. Constr. 42 (2014) 50–67.
[48] F. Vahdatikhaki, A. Hammad, H. Siddiqui, Optimization-based excavator pose estimation using real-time location systems, Automat. Constr. (2015) (accepted for publication).
[49] J. Wang, S.N. Razavi, Low false alarm rate model for unsafe-proximity detection in construction, J. Comput. Civ. Eng. (2015) (available on-line).
[50] S. Worrall, E. Nebot, A probabilistic method for detecting impending vehicle interactions, in: ICRA 2008, IEEE International Conference on Robotics and Automation, IEEE, Pasadena, CA, 2008, pp. 1787–1791.
[51] R.H. Wortman, J.S. Matthias, Evaluation of driver behavior at signalized intersections, Transp. Res. Rec. TRR 1027 (1985) 20–30.
[52] H. Wu, J. Tao, X. Li, X. Chi, X. Hua, R. Yang, S. Wang, N. Chen, A location based service approach for collision warning systems in concrete dam construction, Saf. Sci. 51 (1) (2013) 338–346.
[53] W. Wu, H. Yang, D.A. Chew, S.H. Yang, A.G. Gibb, Q. Li, Towards an autonomous real-time tracking system of near-miss accidents on construction sites, Automat. Constr. 19 (2) (2010) 134–141.
[54] C. Zhang, A. Hammad, Multi-agent approach for real-time collision avoidance and path re-planning on construction sites, J. Comput. Civ. Eng. 26 (6) (2012) 782–794.
[55] G. Zolynski, D. Schmidt, K. Berns, Safety for an autonomous bucket excavator during typical landscaping tasks, New Trends Med. Serv. Robots 20 (2014) 357–368.